Optics Communications 323 (2014) 77–86

Contents lists available at ScienceDirect

Optics Communications

journal homepage: www.elsevier.com/locate/optcom

Multi-faceted digital pyramid wavefront sensor

Vyas Akondi*, Sara Castillo, Brian Vohnsen

Advanced Optical Imaging Group, School of Physics, University College Dublin, Belfield, Dublin 4, Ireland

ARTICLE INFO

Article history:
Received 1 November 2013
Received in revised form
25 February 2014
Accepted 2 March 2014
Available online 13 March 2014

Keywords:
Pyramid wavefront sensor
Wavefront sensing
Adaptive optics
Noise
Hartmann–Shack wavefront sensor
Spatial light modulator

ABSTRACT

The modulated pyramid wavefront sensor is known for its high sensitivity and adjustable dynamic range. The need for mechanically moving parts in a modulated pyramid wavefront sensor can be overcome by using the recently proposed digital pyramid wavefront sensor. In this paper, a digital multi-faceted pyramid wavefront sensor is demonstrated with the use of a reflecting phase-only spatial light modulator. The four-pupil digital pyramid wavefront sensor with 4-facets is extended to 6 and 8-facets. It is noted from the experiments performed under identical low-noise conditions that the performance of the wavefront sensor in terms of the root mean square wavefront error remains nearly the same in cases of four, six and eight pupil configurations. Under the circumstances elucidated here, the results of simulations indicate that in the presence of scatter noise, the pyramid wavefront sensor with greater number of pupils could lead to an improvement over the standard four-pupil pyramid wavefront sensor. Noise from scattering makes the choice of optimal modulation radius critical while sensing in open-loop adaptive optics systems.

1. Introduction

In comparison with a Hartmann–Shack (HS) wavefront sensor [1], the pyramid wavefront sensor is known for its high sensitivity, adjustable dynamic range and an ability to obtain images of higher contrast [2,3], similar to the curvature wavefront sensor [4]. In an aberration-free system, the four facets of a conventional pyramid wavefront sensor deflect the aberrated light beam at the focal plane into four identical pupils. The introduced phase distortions can be reconstructed from the '*x*' and '*y*' wavefront slopes, which are proportional to the *sine* of a linear combination of the normalized pupil intensities [5]. To achieve greater dynamic range and sufficiently effective open-loop operation of the wavefront sensor, there is a need to modulate the light beam with respect to the pyramidal prism [2,6]. The recently proposed digital pyramid wavefront sensor eliminates the need for mechanically moving parts while accommodating modulation, as required in the case of its conventional counterpart [7]. Also, the modulation amplitude can be tuned with ease to attain greater control over sensitivity and dynamic range. Another feature of the digital pyramid wavefront sensor is that the number of facets can be chosen at will to alter the number of pupil images. Related, the roof sensor [8] is yet another modification to the conventional pyramid wavefront sensor, designed to reduce the diffraction effects.

Most common noise sources in wavefront sensors are photon noise, readout noise and scattering noise. Photon noise is the fundamental uncertainty associated with light quantization. Readout noise is usually associated with photon counting ability of detectors and the error involved in converting incident photons to image pixel values. Scattering noise is an external noise that essentially originates from random scatters or in imaging applications where scattering noise from targets is unavoidable [9]. The HS wavefront sensor can be severely affected by noise. An appropriate centroiding algorithm is necessary to precisely estimate the location of HS spots, required to estimate the wavefront accurately [10]. In contrast, the curvature wavefront sensor is less affected by uniform noise [4]. This paper addresses through simulations, the effects of noise in a multi-faceted pyramid wavefront sensor in comparison with its conventional four-pupil counterpart.

An increase in the number of pupils would have a direct influence on the impact of noise and may help to overcome the adverse effects of noise on the accuracy of wavefront sensing in certain applications. The aim of this paper is to demonstrate the feasibility of implementing six-faceted and eight-faceted digital pyramid wavefront sensors using an 8-bit reflecting spatial light modulator and thereby investigate the influence of the increased number of pupils on the performance of the wavefront sensor, in the presence of noise. Adopting a circular modulation scheme, a discussion on the optimum modulation amplitude required to achieve good results in the presence of noise is presented. In order to attain good wavefront sensing accuracy, the aberrated point spread function should be centered precisely on the pyramidal phase addressed on the SLM. A small misalignment near the focal plane could lead to a significant wavefront error analogous to a tilt aberration. A least-square fitting based modal decomposition based on Zernike polynomials is performed after following a

* Corresponding author. Tel.: +353 1 716 2352.
E-mail address: vyas.akondi@ucd.ie (V. Akondi).

http://dx.doi.org/10.1016/j.optcom.2014.03.004
0030-4018

zonal-based wavefront reconstruction procedure. This helps in eliminating tilt-offset errors.

2. Experimental setup

The experimental setup is shown in Fig. 1 and is similar to that used for demonstrating the working of a four-faceted digital pyramid wavefront sensor earlier [7]. A spatially filtered and collimated linearly polarized He–Ne laser (5 mW) was used as source of light. Phase aberrations were introduced in the front focal plane of a 1000 mm focal length achromatic lens using a 140-actuator deformable mirror (DM) from Boston Micromachines™. This long focal length lens was required to avoid overlapping diffraction orders of the pupil images. The SLM (Hamamatsu, LCOS SLM X10468 with a pixel pitch of 20 μm) was placed 1 m away from this lens such that the unaberrated light beam focuses on the SLM display. With the help of a beam splitter, the SLM reflected pupil images (four, six or eight) were captured on a CCD camera. Wavefronts are estimated from the pupil images by adopting the reconstruction approach described in the next section. Concurrently, the aberrations introduced by the DM were sensed using a commercial HS wavefront sensor. The active beam diameter is 4 mm.

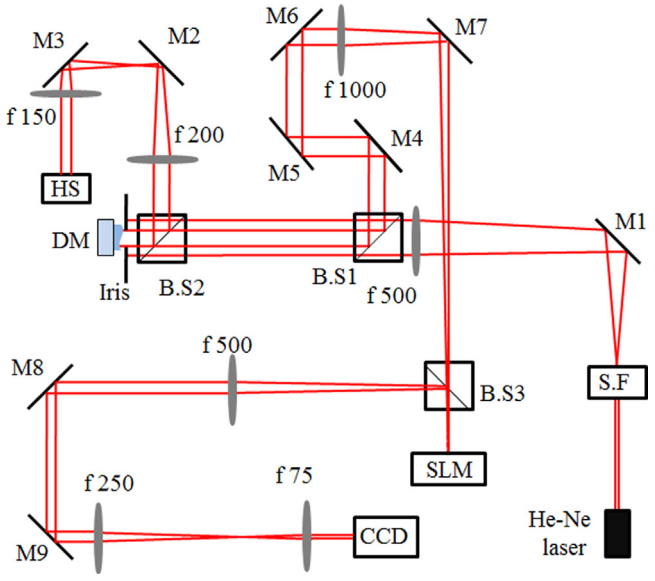

Fig. 1. Schematic of the optical layout for comparison of six and eight pupil configurations with the four pupil digital pyramid wavefront sensor. All the lenses used here are achromatic doublets. S.F is a spatial filter setup, M (1–9) are mirrors and B.S (1–3) are beam splitters. Adapted from [7].

3. Simulations

3.1. Pyramidal phase

Different methods have been used for simulating pyramidal phase in the case of 4-facet pyramid wavefront sensor earlier [7,11–13]. Here, a geometric approach similar to the phase mask approach adopted by Carbillet et al. [13] was used in all three cases for uniformity and easier simulation of 6 and 8-faceted pyramidal phases. Four, six and eight faceted pyramidal phases were generated with the SLM by addressing gray scale values as shown in Fig. 2. Although a greater number of pixels (400×400) were used to simulate the phase in Fig. 2 for perspicuity, an area of 1 mm^2 on the SLM display corresponds to 50×50 SLM pixels. The apex angle of the pyramidal prism was chosen to be $\sim 179^\circ$ such that the area occupied by the pupil images on the CCD camera is optimal. To achieve this apex angle, the pyramidal phase has to be wrapped on the SLM since the maximum non-wrapped phase amplitude of the SLM at 632.8 nm is nearly 3π radians. The high resolution of the SLM allows to safely implement phase wrapping. On the contrary, the need for wrapping the phase on the SLM with square shaped pixels makes it difficult to accurately generate the required phase maps with six and eight facets. The complexity will increase further if more facets are to be introduced. Under the extreme limit, the number of facets is infinite and is analogous to the axicon wavefront sensor [14]. The intensity as measured at the detector plane is given by

$$I^{pyr}_{4,6,8}(x,y) = |FT(FT(C(x,y)\cdot e^{i\phi(x,y)})\cdot e^{iP_{4,6,8}(x,y)})|^2 \quad (1)$$

where $C(x,y)$ defines the circular pupil and $\phi(x,y)$ is the introduced phase aberration. P_4, P_6 and P_8 are the geometrically calculated pyramidal phase functions (see Fig. 2) corresponding to 4, 6 and 8-faceted pyramid wavefront sensors. Here, *FT* represents the fast Fourier transform. To study the effects of noise, a matrix of random numbers picked from a Gaussian distribution is added to the pupil images.

3.2. Wavefront slopes and reconstruction

The analytical dependence of the wavefront slopes on the pupil images in cases of 4, 6 and 8-faceted pyramid wavefront sensors varies due to their fundamental geometrical distinction. Fig. 3 shows the indexing of the pupil geometry together with a reference coordinate system for the wavefront sensor signal to evaluate the relationship between the intensity in the pupils and the wavefront slopes. Following Fig. 3(a), in the 4-facet case, the

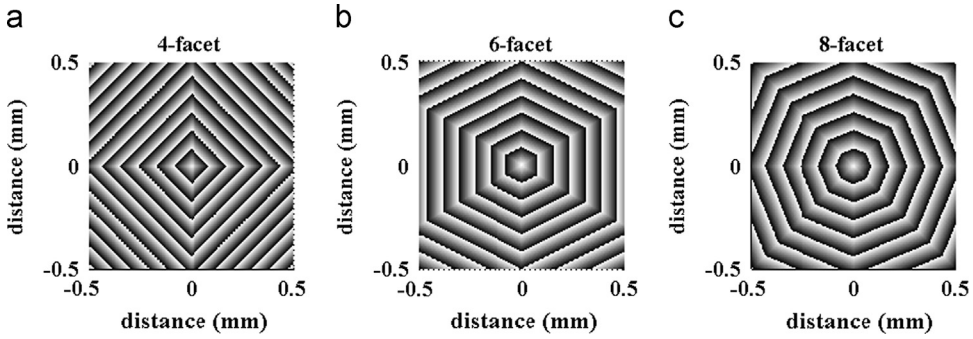

Fig. 2. Wrapped phase addressed on the SLM to generate (a) 4-pupil (b) 6-pupil and (c) 8-pupil pyramid wavefront sensors is shown here. It is to be noted that the phase is over an area of 1 mm^2, corresponding to 50×50 pixels of the SLM. For visualization, 400×400 pixels were used here. The brightest pixel in each map corresponds to a gray value of 255 and the darkest pixel to 0 which corresponds to 3π phase modulation.